5232–5241 *Nucleic Acids Research, 2007, Vol. 35, No. 15* *Published online 2 August 2007*
doi:10.1093/nar/gkm557

Chromosome-specific and noisy *IFNB1* transcription in individual virus-infected human primary dendritic cells

Jianzhong Hu[1], Stuart C. Sealfon[2,3], Fernand Hayot[2,3], Ciriyam Jayaprakash[4], Madhu Kumar[1], Audrey C. Pendleton[1], Arnaud Ganee[1], Ana Fernandez-Sesma[1,3], Thomas M. Moran[1,3] and James G. Wetmur[1,3,*]

[1]Department of Microbiology, Mount Sinai School of Medicine, [2]Department of Neurology, Mount Sinai School of Medicine, New York 10029 USA, [3]Center for Translational Systems Biology, Mount Sinai School of Medicine and [4]Department of Physics, Ohio State University, Columbus, Ohio 43210, USA

Received May 1, 2007; Revised July 2, 2007; Accepted July 7, 2007

ABSTRACT

The induction of interferon beta (*IFNB1*) is a key event in the antiviral immune response. We studied the role of transcriptional noise in the regulation of the *IFNB1* locus in primary cultures of human dendritic cells (DCs), which are important 'first responders' to viral infection. In single cell assays, *IFNB1* mRNA expression in virus-infected DCs showed much greater cell-to-cell variation than that of a housekeeping gene, another induced transcript and viral RNA. We determined the contribution of intrinsic noise by measuring the allelic origin of transcripts in each cell and found that intrinsic noise is a very significant part of total noise. We developed a stochastic model to investigate the underlying mechanisms. We propose that the surprisingly high levels of *IFNB1* transcript noise originate from the complexity of *IFNB1* enhanceosome formation, which leads to a range up to many minutes in the differences within each cell in the time of activation of each allele.

INTRODUCTION

Dendritic cells (DCs) contribute to the non-specific innate immune response to viral infection, as well as to the development of viral antigen-specific adaptive immunity. A salient component of the early DC response to viral infection is the induction of interferon beta (*IFNB1*), a secreted cytokine that complexes with type I IFN receptors to initiate a coordinated cellular program leading to widespread viral resistance (1,2). *IFNB1* expression is a crucial step in both induction of innate immunity and in DCs maturation leading to induction of adaptive immunity. Because the induction of *IFNBI* is so critical for the immune response, the mechanism underlying its control has been the subject of detailed study. The transcriptional activation of the *IFNB1* gene requires the cooperative assembly of a multi-subunit enhanceosome, which includes an AP1 complex, IRF dimers, NFκB (3) and HMGI(Y) (4,5). The crystal structure of several components forming the *IFNB1* enhanceosome has been solved (6).

Pathogenic viruses produce protein antagonists that interfere with the innate immune response, for example by suppressing transcription factor activation and interferon induction. Newcastle disease virus (NDV) is an avian virus that lacks a functioning antagonist in human cells (7–9). Because NDV infection efficiently stimulates the innate immune responses and the maturation of human DCs, it provides an ideal experimental perturbation with which to study unimpeded DC responses to viral infection. To assess the noise in *IFNB1* gene induction, we quantified the variation in gene expression in individual primary human DCs following NDV infection using one-step quantitative reverse-transcription real-time PCR (Figure 1A).

Gene expression noise has a significant effect on many biological processes, such as contributing to phenotypic variability of genetically identical organisms and determining cellular fate following viral infection in bacteria and eukaryotic cells (10–17). Gene noise has been investigated using engineered gene reporters in unicellular organisms (18–23) and has recently been studied in metazoans (24–26). Previous researchers distinguished two components of the total genetic noise to be intrinsic noise and extrinsic noise (21). Intrinsic noise results from the probabilistic nature of molecular processes, such as transcription and translation resulting from the limited number of molecules reacting within an individual cell.

*To whom correspondence should be addressed. Email: james.wetmur@mssm.edu

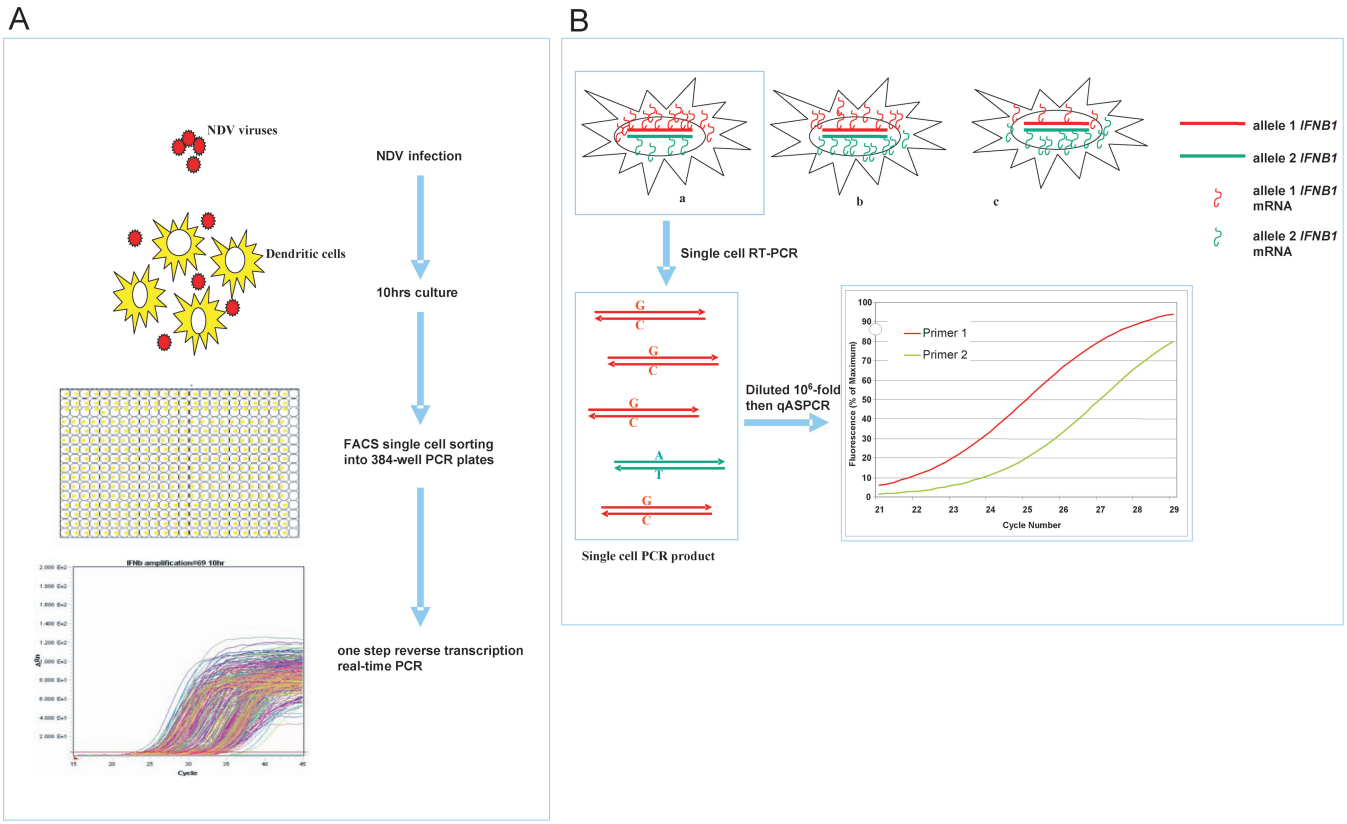

Figure 1. Schematic illustrating the protocol used to measure *IFNB1* mRNA levels synthesized by each allele within individual dendritic cells (DCs). (**A**) Isolation of virus-infected DCs for single cell real-time PCR. NDV viruses (red circles) were co-incubated with monocyte-derived human DCs (yellow). DCs were separated into 384-well PCR plates by visual light scatter using a fluorescent-activated cell sorter (FACS). DCs then underwent single cell one-step reverse-transcription and real-time PCR. The resulting amplification curves from one plate which show fluorescence levels as a function of PCR cycle number are shown for illustration. (**B**) Schematic illustrating the principle of the allelic imbalance assay used to quantify *IFNB1* mRNA synthesized from each allele within individual DCs. mRNA allelic imbalance (AI), defined as the difference between the transcript level from each of the two alleles divided by the sum, can range from −100 to 100%. On average, the same amount of mRNA is synthesized from each of the two *IFNB1* alleles, which are functionally indistinguishable. However, the relative synthesis from each allele within each cell can vary as a result of intrinsic noise. a, b and c represents individual DCs in which *IFNB1* is synthesized mostly from one allele, equally from both alleles, or mostly from the other allele, respectively. The curly lines within each DC represent the *IFNB1* mRNA molecules and their color (red or green) indicates their origin from one or the other allele. The mRNAs differ by a single nucleotide and the amplified single cell PCR product preserves their relative levels of expression within each cell. Each single cell PCR product was then subjected to a second allele-specific PCR reaction (ASPCR) that measured the relative levels of *IFNB1* expression from each allele based on the single nucleotide difference. The graph illustrates the difference in the plots obtained from a single cell with differential expression from the two alleles. A detailed explanation of the methodology is found in Methods section.

Extrinsic noise results from cell-to-cell variations in components involved in generating the response. Total noise is the contribution of both processes to cell-to-cell variation.

Previous studies of noise have largely utilized protein reporter assays, which add translational noise to the data generated as well as measurement noise due to cellular autofluorescence and other limitations of direct fluorescence assays. In our experiments, we directly measured single cell *IFNB1* mRNA expression in order to characterize the total noise of *IFNB1* induction following virus infection of human dendritic cells (DCs). We employed a new real-time RT-PCR-based approach for quantification of transcripts. After virus infection, single DCs were screened and sorted directly into 384-well PCR plates, which contained cell lysis buffer and RNAse inhibitor in each well. One-step real-time reverse transcription PCR was performed and the total number of *IFNB1* transcripts in each cell were measured. To determine the intrinsic components of total noise, we measured the differential expression from two alleles of heterozygous human DCs, using a common readout polymorphism of *IFNB1* (rs1051922). The method of measurement utilized a second qRT-PCR (for details see Figure 1B and Methods section) (27).

Our results show a considerable cell-to-cell variability of *IFNB1* gene expression, of which intrinsic noise is a significant component. Intrinsic noise cannot be due to cell-to-cell fluctuations in viral load, the number of transcription factors, signaling components or polymerases, since these would affect both alleles equally in a given cell. The source of intrinsic noise must lie within the transcription process itself, and therefore is likely associated with the complexity of enhanceosome assembly

on the *IFNB1* promoter (28). The single cell model we have developed to interpret our results on *IFNB1* noise is based on the premise that intrinsic noise and therefore allelic imbalance results precisely from the stochasticity of enhanceosome formation.

METHODS

Differentiation of DCs

All human research protocols for this work have been reviewed and approved by the IRB of the Mount Sinai School of Medicine. Monocyte-derived DCs were obtained from healthy human blood donors following a standard protocol as described elsewhere (29). Briefly, human peripheral blood mononuclear cells were isolated from buffy coats by Ficoll density gradient centrifugation (Histopaque, Sigma Aldrich) at 2300 r.p.m. and $CD14^+$ monocytes were immunomagnetically purified by using a MACS CD14 isolation kit (Miltenyi Biotech). Monocytes (0.7×10^6 cells/ml) were differentiated into immature DCs by 5–6 day incubation in 1 ml DC growth media with RPMI Medium 1640 (Invitrogen/Gibco) supplemented with 10% fetal calf serum (Hyclone), 2 mM of L-glutamine, 100 U/ml penicillin and 100 g/ml streptomycin (Pen/Strep) (Invitrogen), 500 U/ml hGM-CSF (Preprotech) and 1000 U/ml hIL-4 (Preprotech).

Virus preparation and viral infection

The recombinant Hitchner strain of Newcastle disease virus (rNDV/B1) was prepared as described by Park *et al.* (30). Aliquots of allantoic fluid were harvested, snap frozen and stored at −80°C. All virus preparations were free of bacterial contamination, as tested by the inoculation of blood agar plates. NDV virus was titered by immunofluorescence 18 h after infection of Vero cell plates using monoclonal antibodies specific for NDV HN protein (Mount Sinai Hybridoma Core Facility) followed by addition of anti-mouse IgG-FITC and visualization using fluorescent microscopy. NDV stocks were appropriately diluted in Dulbecco's Modified Eagle Medium (DMEM) and added directly into pelleted DCs at a multiplicity of infection (MOI) of 0.5 (31). After incubation for 40 min at 37°C, fresh DC growth medium (without GMCSF and IL-4) was added back to the infected cells (1×10^6 cells/ml) for the remainder of the infection. Virus-free allantoic fluid was added to additional tubes of cells to serve as a negative control.

Measurement of *IFNB1* mRNA lifetime

Cultured human DCs (1×10^6 cells) were divided into two samples (5×10^5 cells each). Cells in both samples were infected by NDV at an MOI of 0.5, and actinomycin D was added at 5 μg to one sample 9 h after virus infection to inhibit transcription. Total RNA samples were isolated using a Qiagen RNeasy mini kit every half an hour from 10 h through 12 h. The concentrations of RNAs were determined using a Nanodrop® ND-1000 Spectrophotometer. One hundred nanogram of each RNA sample was used as template for qRT-PCR to determine the expression levels of *IFNB1* and *TNF*. The data were normalized to *ACTB*, *TUBA1B* and *RPS11*. All PCR primer sequences are given in Supplementary Table 1.

Single DC sorting

Virus infected DCs were resuspended on ice in PBS at a concentration of $2–5 \times 10^5$ cells/ml. Cells were filtered through a 50 μm filter to remove aggregates prior to FACS (fluorescence activated cell sorting) sorting. Single DC was screened and sorted by visual light scatter (MoFlo high speed cell sorter) directly into 384-well bar-coded PCR plates (Applied Biosystems), which contained 5 μl cell lysis buffer [4 mM magnesium acetate (Sigma), 0.05% NP40 (Sigma), 0.8 U/μl Protector RNAse Inhibitor (Roche Applied Sciences)] in each well. Sorted DCs were immediately placed on dry ice and stored at −70°C to prevent RNA degradation.

Single DC real-time RT-PCR

One-step real-time reverse transcription PCR was performed on an ABI PRISM 7900HT sequence detection system (SDS) (Applied Biosystems) based on the manufacturer's recommended standard protocol except for cycling conditions. Following incubation at 65°C for 30 min, as required for the reversed transcription step, amplification was carried out for 50 cycles using 95°C for 30 s and 60°C for 30 s. The one-step protocol was made possible by using AccuRT, an aptamer-based hot-start, magnesium-activated thermostable DNA polymerase that extends a primer on either an RNA or DNA template (32). An aliquot of 5 μl of 2× PCR reaction mix [2× buffer, 4 mM magnesium acetate, 1 μM each primer, 0.4 mM each dNTP (0.8 mM dUTP replacing dTTP) and 0.375 U/μl AccuRT with aptamer (provided by Roche Molecular Systems; research samples of this polymerase may be obtained from Dr Thomas Myers (thomas.myers@roche.com)] was added into each well of a FACS single cell-sorted 384-well PCR plate using a multichannel pipettor. *IFNB1* mRNA, *DDX58* mRNA, control gene ribosomal protein 9 (*RPL9*) mRNA or NDV L gene RNA in each cell was directly amplified into 106, 156, 76 and 125 bp amplicons, respectively (primers' sequences are found in Supplementary Table 1). At the end of each reaction, crossing threshold (Ct) was determined at a manually adjusted level that reflected the best kinetic PCR parameters, and melting curves were acquired and analyzed to validate the products. The number of transcripts in each cell was determined by relating the Ct value to the standard curve for the corresponding gene.

Allele-specific PCR

IFNB1 and control gene *RPL9* were genotyped at selected readout SNPs (rs1051922 for *IFNB1*, rs1065744 for *RPL9*) and DCs from heterozygotes were selected for single cell analyses. *IFNB1* and *RPL9* amplicons from single cell real-time PCR measurements were used as templates to quantify the amplification from the two alleles using allele-specific PCR (ASPCR) (27). ASPCR uses one common primer and a second allele-specific

primer based on the 3′ nucleotide. Allelic imbalance (AI) is defined as the difference in the number of transcripts from the two alleles (M1−M2) divided by the total transcripts (M1 + M2), expressed as percentage. This difference was calculated based on the differences in Ct values (ΔCt) for the two allele-specific primers.

$$\mathrm{AI}\% = \frac{(1 - 2^{\Delta \mathrm{Ct}})}{(1 + 2^{\Delta \mathrm{Ct}})} \times 100\%$$

This ASPCR assay was performed on an ABI PRISM 7900HT SDS (Applied Biosystems). Single cell reverse-transcriptase PCR products were pre-selected by melting curve screening to eliminate those containing primer–dimer and diluted 1:10^6. Five microliter dilutions were added as template into the reaction mix of equal volumes as described elsewhere (33) [100 mM Tricine buffer, pH 7.5, 100 mM KOAc, 16.0% glycerol, 2% dimethyl sulfoxide, 0.4 mM dATP, dCTP and dGTP, 0.8 mM dUTP, 6 mM magnesium acetate, 2× SYBR Green (Invitrogen), 1.0 μM primers, 0.4 Unit ΔZ05 GOLD DNA Polymerase (a Hotstart DNA polymerase with improved discrimination against misextension kindly provided by Roche Molecular Systems; research samples of this polymerase may be obtained from Dr Thomas Myers (thomas.myers@roche.com)] in 384-well-format PCR plates. The cycling conditions were 95°C for 12 min to activate the polymerase, 40 cycles of 30 s at 95°C, 30 s at 58°C and 30 s at 72°C. In an alternative PCR buffer [50 mM Tris buffer, pH 7.5, 50 mM KOAc, 2% glycerol, 1× BSA (0.1 mg/ml)], other hot-start Taq DNA polymerases perform well in ASPCR, but not as well as ΔZ05 (data not shown). ASPCR for *IFNB1* and *RPL9* produces 66 and 59 bp amplicons, respectively, using the primers listed in Supplementary Table 1. All assays were replicated and normalized against heterozygote DNA as previously described (27).

Measurement accuracy and individual variation

The systematic error of our measurements was determined by performing the entire qRT and ASPCR steps using serial dilutions of total RNA extracted from NDV-infected DCs from a single heterozygous donor as reaction templates. Total RNA was diluted from 5000 copies to 19 copies per qRT reaction. Twelve PCR products from each dilution were then used as the template for the ASPCR assays.

Single cell multiplex TaqMan assay

A multiplex single cell TaqMan assay has been established to study the correlation between the level of NDV L gene and *IFNB1* transcription in single human DCs. The one-step real-time reverse-transcription-TaqMan assay was performed in single DCs by using AccuRT as described above for single cell real-time RT-PCR with the only variation being 0.4 μM primer pairs and 0.6 μM TaqMan probes and the absence of SYBR Green. The sequences of the primer sets and TaqMan probes for *IFNB1* mRNA (FAM labeled) and NDV L gene (HEX labeled) are listed in Supplementary Table 1.

Stochastic model

The model is based on the premise that the observed noise in *IFNB1* mRNA is a result of stochasticity in the time of onset of transcription. More precisely, the complexity of *IFNB1* enhanceosome formation prior to transcription initiation is assumed to provide the dominant contribution to the stochastic behavior. This assembly involves binding of the transcriptional activators, the heterodimers NFκB and AP-1 (ATF-2-c-Jun) and the interferon regulatory factors IRF to form the enhanceosome (6) as well as the architectural protein HMG-I(Y) (4,34–36). If these proteins bind weakly to their promoter region (19,22), the time at which enhanceosome formation is complete fluctuates between alleles in a given cell, providing a source of intrinsic noise. Once stabilized, the enhanceosome is assumed to persist and stimulate transcription during the course of the experiment. The complex processes that occur once the enhanceosome is stabilized, including the building of the Pol II complex etc., are not explicitly included and only a stochastic transcription of mRNA production is modeled.

For simplicity, in the following description of the model we will denote HMG-I(Y) by P1, NFκB by P2, AP1 by P3 and the IRFs by P4. The model thus comprises four proteins P1, P2, P3 and P4 that bind without interacting, as indicated by experiment (6). Since the binding occurs through DNA conformational changes (6), we represent the corresponding cooperative behavior through protein binding in a well-defined order. While more than one IRF factor may be required and two HMGI-(Y)s are needed, we include just four reactions in our simple model, since these account reasonably for the combinatorial nature of the sequential, cooperative assembly and consequent stochasticity in the time of transcription initiation. Since the experiment measures AI, we distinguish enhanceosome binding to either allele.

The relevant reactions are given by:

$$D1 + P1 \underset{k2}{\overset{k1}{\leftrightarrow}} Ds1$$

$$Ds1 + P2 \underset{k4}{\overset{k3}{\leftrightarrow}} Ds11$$

$$Ds11 + P3 \underset{k6}{\overset{k5}{\leftrightarrow}} Ds12$$

$$Ds12 + P4 \overset{k7}{\rightarrow} Ds13$$

where $D1$ represents promoter region of allele 1. One has a similar set of equations for promoter region $D2$ of allele 2 where we have used the same reaction rate constants since the alleles are assumed to be functionally identical. Once the enhanceosome is bound (complex $Ds13$ and the corresponding complex for allele 2), transcription proceeds according to a Poisson process at the rate of ten mRNA molecules of *IFNB1* per minute for both allele 1 and allele 2. Transcription itself is thus noisy; we have checked that this makes a small contribution to AI (intrinsic noise), which is dominated by fluctuations in the time of transcription initiation. The transcription by the gene in allele 1 is represented simply by:

$$Ds13 \overset{tr}{\rightarrow} Ds13 + mRNA1.$$

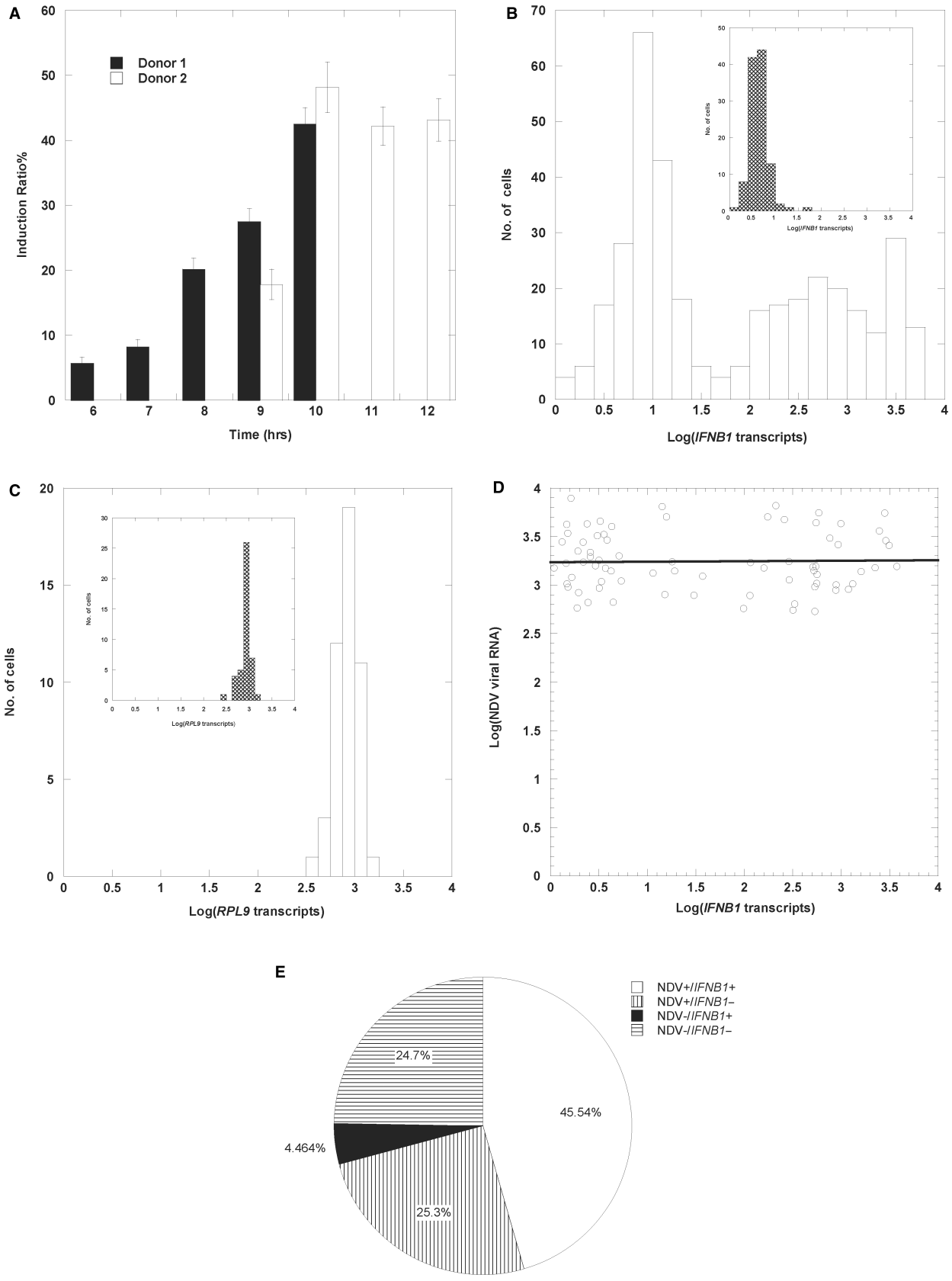

Figure 2. Single cell analysis of gene expression in NDV-infected human DCs. All infections were carried out at viral multiplicity of infection (MOI) = 0.5. Non-infected (NI) single cells were analyzed as a negative control. (**A**) The induction ratio is the percentage of cells showing induction of *IFNB1*. Shown are the *IFNB1* induction ratios obtained in DCs that were exposed to NDV for varying times (6–12 h) from two donors. The data

We have also included the decay of the mRNA both simply as a decay process where mRNA decays very rapidly after 3 h, as indicated by experiment, and a multi-step process to account for the poly (A) tail degradation that precedes the degradation of the mRNA.

Experimental measurements are made on single cells, not across a population. Therefore, we have employed the well-known Gillespie algorithm to simulate AI (37). In the algorithm, the time intervals between reactions is chosen from an exponential distribution and the reactions themselves are chosen randomly according to weights that are proportional to rate constants and number of particles involved in the reaction.

Since measurements of the amounts of enhanceosome components do not exist, we take for simplicity the initial numbers of P1, P2, P3 and P4 to be equal to 12 000, which for a volume of $500\,\mu^3$ corresponds to a concentration of 40 nM. Within the implementation of the model, the rate constants and the corresponding copy numbers of the transcription factors enter as products and thence, independent specification of the two numbers is not crucial. For reasons of simplicity as well we take all the binding constants to be equal and given by $k1 = k3 = k5 = k7 = 4.85 \times 10^{-5}\,\mathrm{nM}^{-1}\,\mathrm{s}^{-1}$, and the unbinding constants are equal and given by $k2 = k4 = k6 = 24.25 \times 10^{-4}\,\mathrm{s}^{-1}$. We have also tried varying the rate constants within factors of 1/5 to 5 preserving the overall timescale and find that our results are robust at the semi-quantitative level.

There is an additional time delay between the initial infection and the subsequent formation of active transcription factors due to a number of steps: the viral RNA being presented to the cell, the activation and nuclear translocation of NFκB from its sequestered form by ubiquitination of IκB and activation of the other transcription factors. The experimental measurements, which show a strong component of extrinsic noise (see legend of Figure 3), suggest this directly since for different cells virus-induced transcription of *IFNB1* mRNA starts at different times, with most cells being active after 8 h of viral infection, but some cells starting transcription hours earlier. To account for this, the starting time of chemical reactions in the model is chosen from a Gaussian distribution centered at 6 h with a width of 1 h, with the requirement that no cell starts transcription within 4 h of viral infection. We have also modeled a cascade of processes separately and parameterized the probability distribution for the time delay before the starting time for the reactions of our model as a Gamma distribution. The results obtained are quantitatively similar.

RESULTS AND DISCUSSION

Noisy *IFNB1* induction by viral infection in primary human DCs

To maximize the fraction of infected cells while minimizing the number of cells infected by multiple viruses, experiments were performed at an infectious particles/cell ratio [multiplicity of infection (MOI)] below one. To select the time points for studying noise, we determined the fraction of cells expressing *IFNB1* at various times following NDV infection. After NDV infection, the number of cells expressing *IFNB1* increased between 6 and 10 h and plateaued at ~10 h (Figure 2A). Because the *IFNB1* gene lacks introns, the PCR reaction cannot discriminate between the four strands of genomic DNA in each cell and the transcribed *IFNB1* mRNA. Therefore a low level of *IFNB1* signal was detected in the absence of viral infection (Figure 2B inset). In contrast, the virus-exposed cells showed a second broad distribution of expression levels resulting from highly variable single cell *IFNB1* induction (Figure 2B). We also determined the individual cell-to-cell expression of a constitutively expressed housekeeping gene (*RPL9*) as well as of an additional virus-induced gene *DDX58* (RIG-I). In contrast with *IFNB1* in activated cells, *RPL9* showed a narrow distribution indistinguishable in infected and uninfected cells (Figure 2C). Like *RPL9*, the virus-induced *DDX58* mRNA also showed a narrow distribution (Supplementary Figure 1). The measurement of *RPL9*, which also served to assess the efficiency of sorting of single, viable cells, revealed only 2% measurement failure due to sorting errors.

Stochasticity of *IFNB1* induction is not determined by the stochastic nature of viral RNA replication

In a separate experiment, we used a single cell multiplex TaqMan assay to determine the covariation in expression of *IFNB1* mRNA and NDV viral RNA. Regression analysis showed that the level of *IFNB1* mRNA was independent of the level of NDV replication in the same cell (Figure 2D). Furthermore, approximately one-third of the cells infected with virus, as shown by expression of NDV viral RNA, showed no significant induction of *IFNB1* (Figure 2E). Reflecting the high levels of cell-to-cell

were obtained by cell sorting and single cell mRNA expression measurements as illustrated in Figure 1A. The two donors were sampled at different time points because practical considerations limit the number of samples that can be sorted and assayed in any single experiment. (**B** and **C**) Histograms showing gene expression level in logarithmic scale. The histograms represent the entire population of cells studied, with each measurement obtained from a different cell. The results obtained in control cells (inset) and in NDV infected cells are compared in each panel. (**B**) Histogram of *IFNB1* expression at 10 h from one donor. The second broad peak of infected cells shows an elevated *IFNB1* mRNA expression induced by viral infection. (**C**) Histogram of ribosomal protein gene 9 (*RPL9*), a housekeeping control gene, at 10 h from the same donor as in B and C above. Viral infection has no effect on *RPL9* mRNA level. (**D**) Multiplex analysis of single cell *IFN*β and NDV viral mRNA expression. The data shown in the graph were obtained using a different donor than the data shown in panels B and C. The NDV L gene, located at the 5′ end of NDV viral genomic RNA, is the last to be transcribed and is the least abundant. Thus its detection by PCR is the most accurate measurement of the level of viral RNA. The levels of viral RNA and *IFNB1* mRNA within each DC were uncorrelated. (**E**) Pie chart of populations of cells expressing NDV and *IFNB1* (NDV+/*IFNB1*+), *IFNB1* alone (NDV−/*IFNB1*+), NDV alone (NDV+/*IFNB1*−), and neither (NDV−/*IFNB1*−). NDV+ indicates that viral RNA was detected by the L gene PCR reaction.

variation in *IFNB1* mRNA in NDV-infected cells, we find that 7% of infected cells accounted for more than 50% of all *IFNB1* mRNA synthesized (Figure 2B). These findings show that the stochasticity of *IFNB1* expression is not determined by the stochastic nature of viral RNA replication. It must therefore result from heterogeneity in individual DCs' responses to virus infection and the process of *IFNB1* transcription. We also found that some cells expressed *IFNB1* mRNA in the absence of evidence of viral RNA replication. This may be due to the presence of undetected defective interfering particles in the NDV viral stock (9).

Stability of *IFNB1* mRNA

IFNB1 RNA is stable for at least 2 h after synthesis, until the poly (A) tail is removed and exponential degradation commences (38,39). To confirm the kinetics of degradation in DCs, control studies were performed by adding actinomycin D 9 h after NDV infection, thus inhibiting transcription. *IFNB1* mRNA levels were found to be stable for more than 2 h after actinomycin D treatment, followed by a rapid decay phase (Supplementary Figure 2A). *TNF* degradation, which showed exponential decay immediately after addition of actinomycin D, served as a control (Supplementary Figure 2B). Coupled with the fact that *IFNB1* mRNAs were mainly synthesized 8 h after NDV infection (Figure 2A), these results indicate that the effects of degradation of *IFNB1* mRNA on its level of expression do not affect the interpretation of the single cell assays.

Intrinsic noise in individual DCs

Experiments were performed using DCs from individuals heterozygous for the *IFNB1* readout polymorphism, which enabled mRNA from each of the two alleles to be distinguished. We quantified the level of single cell *IFNB1* production by qRT-PCR (Figure 1A). We also quantified the relative number of transcripts measured from each allele within each cell by allele-specific PCR (Figure 1B). mRNA allelic imbalance (AI) is the difference in mRNA production from the two alleles divided by their sum (40) and is directly calculated from the ΔCt values for replicate allele-specific PCR reactions (see Methods section). The number of transcripts originating from each of the two alleles (M1, M2) was calculated from the total expression and AI for each cell (see Methods section).

We verified the equality of the distributions of M1 and M2 by a Kolmogorov–Smirnov test ($P = 0.23$ at 8 h, $P = 0.99$ at 9 h, $P = 0.46$ at 10 h). At low single cell expression levels, the majority of cells showed expression from one or the other allele at 8, 9 and 10 h after infection (Figure 3A–C). When *IFNB1* mRNA expression was greater, most cells showed expression from both promoters. Because these experiments use primary cells, studies were replicated using cells from different donors in order to assess the robustness of the distributions found. The distributions seen in Figure 3A–C are comparable to those obtained in other experiments (Supplementary Figure 3). The running average of the absolute value of the difference between *IFNB1* transcripts from the two alleles ($\langle|M1 - M2|\rangle$) was calculated and plotted versus the running average of the total transcripts ($\langle|M1 + M2|\rangle$) (Supplementary Figure 4). The similarity of these plots representing different times after infection suggests that the intrinsic noise in *IFNB1* (shown by ($\langle|M1 - M2|\rangle$) depends on the total *IFNB1* transcription and is not dependent on time elapsed since viral infection.

In order to quantify the noise, we used the definitions proposed by Elowitz *et al.* (21). In brief, if M1 and M2 designate the numbers of *IFNB1* mRNA transcripts from the two alleles, intrinsic noise η_{int}, extrinsic noise η_{ext} and total noise η_{tot} are given by:

$$\eta_{\text{int}}^2 = \frac{\langle (M1-M2)^2 \rangle}{2\langle M1 \rangle \langle M2 \rangle}$$

$$\eta_{\text{ext}}^2 = \frac{\langle M1\,M2 \rangle - \langle M1 \rangle \langle M2 \rangle}{\langle M1 \rangle \langle M2 \rangle}$$

$$\eta_{\text{tot}}^2 = \eta_{\text{int}}^2 + \eta_{\text{ext}}^2$$

where the brackets ($\langle\ \rangle$) denote averages over all activated cells. The level of total noise reflected in the level of single cell expression (Figure 2B) and the level of intrinsic noise reflected by the level of single cell AI were high, with intrinsic noise making a large contribution to total noise (e.g. $\eta_{\text{int}} = 1.4$, $\eta_{\text{ext}} = 2.0$, $\eta_{\text{tot}} = 2.5$ at 8 h). Total and intrinsic noise for the housekeeping control gene *RPL9* were much less than those observed for *IFNB1* (Figure 3D). We determined the accuracy of single cell allelic imbalance assays by simulating single cell experiments using dilutions of mRNA isolated from a large number of DCs. These assays showed that the AI standard deviation resulting from measurement error was much lower than the variation measured for *IFNB1* mRNA, and that the error was independent of the initial copy number down to fewer than 20 target mRNA copies/cell (Supplementary Figure 5).

Stochastic model of *IFNB1* gene activation

The experimental results showed that, in comparison with the other two genes studied, a high level of intrinsic and total noise was observed for *IFNB1* mRNA expression. The high levels of single cell AI observed are incompatible with a model involving transient activation and reactivation of the *IFNB1* promoters. If the *IFNB1* enhanceosome could assemble, activate, disassemble and reactivate on a short timescale relative to these experiments, then the mRNAs originating from each promoter would equalize and single cell AI would not be observed. Therefore, we hypothesized that the differences in M1 and M2 result from differences in the initial formation of each functional *IFNB1* transcription complex. To test this hypothesis, we explored whether a minimal stochastic model based on these assumptions would explain the single cell *IFNB1* mRNA AI levels.

We simulated enhanceosome assembly and mRNA synthesis using Gillespie's algorithm (37). The model we considered is based on the premise that the observed AI results from fluctuations in the time of formation of the

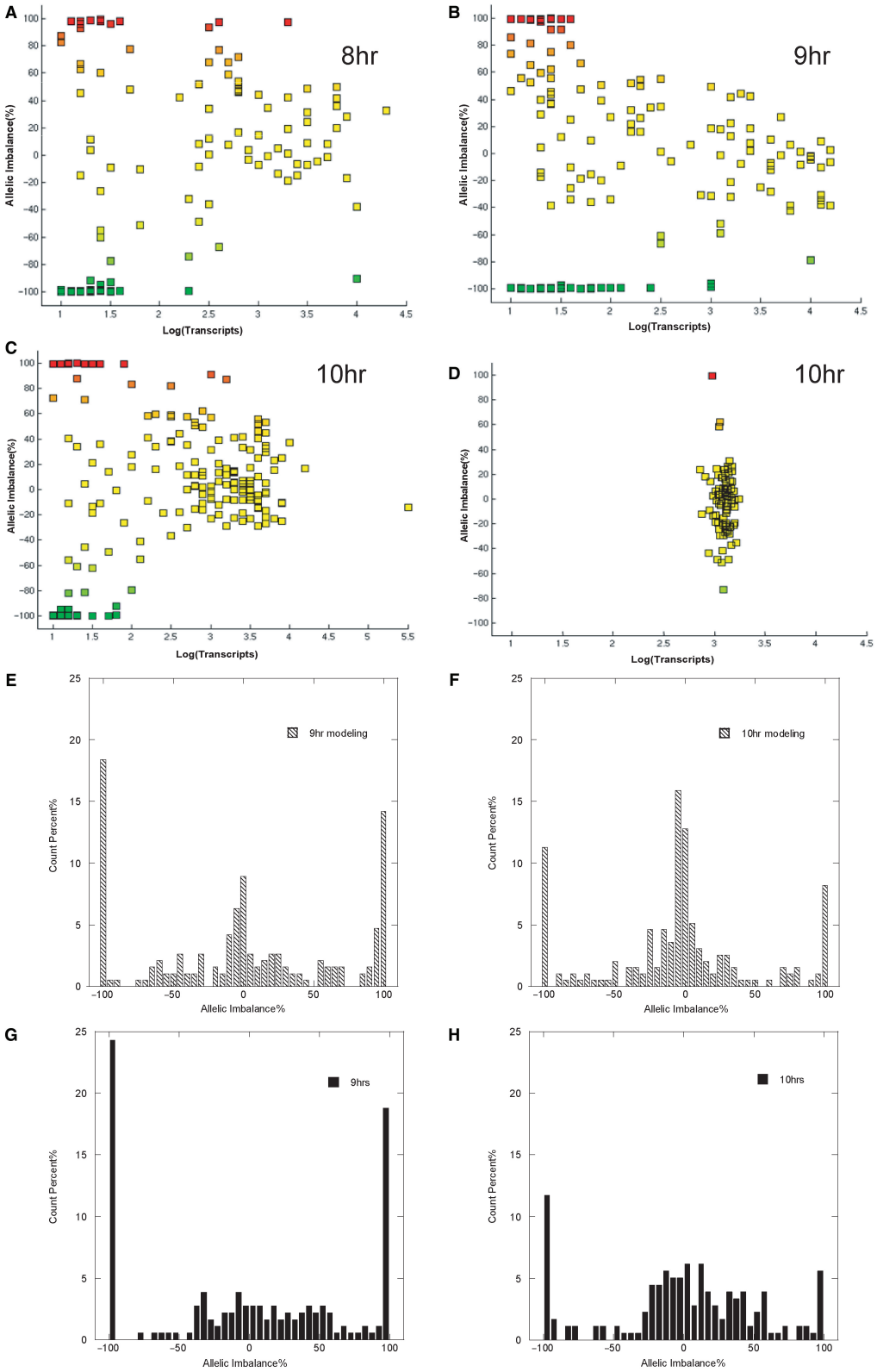

Figure 3. Allelic imbalance (AI) in individual DCs. (**A–C**) Measurement of *IFNB1* AI as a function of total transcript number for individual DCs exposed to NDV at 8, 9 and 10 h. (**D**) Measurement of AI of control gene *RPL9* at 10 h. The color changes from green to yellow to red are set as a function of the relative mRNA expression from the two alleles. Intrinsic noise (η_{int}), extrinsic noise (η_{ext}) and total noise (η_{tot}) were determined as described in Supplementary Data. The results for *IFNB1* were $\eta_{int} = 1.4$, $\eta_{ext} = 2.0$, $\eta_{tot} = 2.5$ at 8 h; $\eta_{int} = 0.6$, $\eta_{ext} = 1.8$, $\eta_{tot} = 1.9$ at 9 h; $\eta_{int} = 0.6$, $\eta_{ext} = 1.3$, $\eta_{tot} = 1.5$ at 10 h; and for control *RPL9* were $\eta_{int} = 0.3$, $\eta_{ext} = 0.0$, $\eta_{tot} = 0.3$. (**E–H**) Histogram of percent of cells showing different levels of AI for *IFNB1* in single human DCs at 9 and 10 h after infection. (**E**) Stochastic model simulation at 9 h. (**F**) Stochastic model simulation at 10 h. (**G**) Experimental results at 9 h. (**H**) Experimental results at 10 h. For details of the model, see Methods section.

enhanceosome complex. These fluctuations produce variability in the time when transcription of *IFNB1* starts on each allele. The differences observed experimentally in M1 and M2 in individual cells suggest that the activation of the second allele is delayed by a period up to many minutes (Figure 3A–C). The intricate series of processes leading up to the beginning of transcription are modeled as a sequence of ordered, slow binding of four proteins, NFκB, IRF3 dimer, AP1 and HMGI(Y), to the enhancer–promoter region of the *IFNB1* gene. The proteins occur in adequate numbers so that their binding to the two alleles is uncorrelated. Single cell AI essentially results from fluctuations in the time of initiation of transcription. Once transcription starts, it continues unabated according to a Poisson process, and does not contribute significantly to the intrinsic noise. The model also incorporates variability in the time elapsed between virus infection and activation of enhanceosome components. This source of cellular variability affects the two alleles in a cell in the same way and does not contribute to intrinsic noise. The distribution of single cell AI reproduces the salient features of the measurements obtained experimentally as the comparison between model and experiment at two different time points shows (Figure 3E–H). The model simulations were robust to a 25-fold variation in the rate constants (see Methods section). These results support the hypothesis that the sequential assembly of the multicomponent enhanceosome represents a major source of intrinsic noise in this system.

The AI (intrinsic noise) determined by simulations of the model and by experimental measurement show a close correspondence (Figure 3E–H). However, the present simple model is far from complete as far as the sources of cell-to-cell variation (extrinsic noise) that lead to activation of the enhanceosome components are concerned. It only gives a qualitative description of the experimental results for total single cell *IFNB1* mRNA yield (compare Figure 3A–C and Supplementary Figure 6). Refinements of the model and further experiments will be necessary to clarify the extrinsic noise mechanisms contributing to cell-to-cell variability in the levels of *IFNBI* mRNA.

Conclusions

The high level of variation in *IFNB1* expression from cell to cell is influenced both by intrinsic stochastic processes and by extrinsic cell-to-cell variation in the initial concentrations of key signaling and enhanceosome components. The lack of correlation between single cell viral RNA and *IFNB1* mRNA expression levels suggested that differences in viral replication do not contribute to the observed variability in *IFNB1* induction. Variation of recruitment of RNA polymerase after enhanceosome formation is also not a significant contributor to the differences in single cell levels of *IFNB1* since the level of housekeeping gene such as *RPL9* is tightly controlled across cells. The measurement of single cell AI provided an assessment of the level of intrinsic noise, as both promoters in each cell are exposed to the same environment. Transient differences in the rate of promoter recruitment or of RNA synthesis are likely to contribute little to the *IFNB1* intrinsic noise, because any imbalances in transcription rate would average out over the timescale of these experiments. Our experimental data and simulations thus suggested that the intrinsic and extrinsic noise contributing to variations in *IFNB1* expression result from variations in the time of formation of the functional *IFNB1* enhanceosome.

The level of *IFNB1* induction in DC cells responding to viral infection is very broad, ranging from few tens to several thousands of mRNA copies. A major element of this cell-to-cell variability is intrinsic noise, which we measured through a readout polymorphism. Our work is the first to measure cell-to-cell variability on *IFNB1* gene expression in human DCs responding to virus infection. Its implication for differential immunity at the population level is unknown. We speculate that high levels of *IFNB1* noise may possibly contribute to the overall robustness of the human antiviral response. Our experimental results show that only a few cells respond strongly to viral invasion. This limited response may be adequate to prime the immune system while at the same time avoiding the overreaction of a cytokine storm. The beneficial, neutral or detrimental effects of the *IFNB1* noise on the overall immune system response to viral infection remain to be established by further studies.

SUPPLEMENTARY DATA

Supplementary Data are available at NAR Online.

ACKNOWLEDGEMENTS

This work was supported by contract HHSN266200500021C and grant U19 AI06231 from the National Institute of Allergy and Infectious Diseases. We thank the Mount Sinai flow cytometry shared research facility for single cell sorting and the Mount Sinai real-time PCR shared research facility. We thank Roche Molecular Systems for generously providing AccuRT and ΔZ05 DNA polymerases. Funding to pay the Open Access publication charges for this article was provided by NIAID.

Conflict of interest statement. None declared.

REFERENCES

1. Kawai,T. and Akira,S. (2006) Innate immune recognition of viral infection. *Nat. Immunol.*, **7**, 131–137.
2. Theofilopoulos,A.N., Baccala,R., Beutler,B. and Kono,D.H. (2005) Type I interferons (alpha/beta) in immunity and autoimmunity. *Annu. Rev. Immunol.*, **23**, 307–336.
3. Covert,M.W., Leung,T.H., Gaston,J.E. and Baltimore,D. (2005) Achieving stability of lipopolysaccharide-induced NF-kappaB activation. *Science*, **309**, 1854–1857.
4. Munshi,N., Agalioti,T., Lomvardas,S., Merika,M., Chen,G. and Thanos,D. (2001) Coordination of a transcriptional switch by HMGI(Y) acetylation. *Science*, **293**, 1133–1136.
5. Klar,M. and Bode,J. (2005) Enhanceosome formation over the beta interferon promoter underlies a remote-control mechanism mediated by YY1 and YY2. *Mol. Cell. Biol.*, **25**, 10159–10170.

6. Panne,D., Maniatis,T. and Harrison,S.C. (2004) Crystal structure of ATF-2/c-Jun and IRF-3 bound to the interferon-beta enhancer. *EMBO J.*, **23**, 4384–4393.
7. Honda,K., Sakaguchi,S., Nakajima,C., Watanabe,A., Yanai,H., Matsumoto,M., Ohteki,T., Kaisho,T., Takaoka,A. *et al.* (2003) Selective contribution of IFN-alpha/beta signaling to the maturation of dendritic cells induced by double-stranded RNA or viral infection. *Proc. Natl Acad. Sci. USA*, **100**, 10872–10877.
8. Park,M.S., Shaw,M.L., Munoz-Jordan,J., Cros,J.F., Nakaya,T., Bouvier,N., Palese,P., Garcia-Sastre,A. and Basler,C.F. (2003) Newcastle disease virus (NDV)-based assay demonstrates interferon-antagonist activity for the NDV V protein and the Nipah virus V, W, and C proteins. *J. Virol.*, **77**, 1501–1511.
9. Lopez,C.B., Yount,J.S. and Moran,T.M. (2006) Toll-like receptor-independent triggering of dendritic cell maturation by viruses. *J. Virol.*, **80**, 3128–3134.
10. Arkin,A., Ross,J. and McAdams,H.H. (1998) Stochastic kinetic analysis of developmental pathway bifurcation in phage lambda-infected Escherichia coli cells. *Genetics*, **149**, 1633–1648.
11. Pascal,V., Stulberg,M.J. and Anderson,S.K. (2006) Regulation of class I major histocompatibility complex receptor expression in natural killer cells: one promoter is not enough! *Immunol. Rev.*, **214**, 9–21.
12. McAdams,H.H. and Arkin,A. (1997) Stochastic mechanisms in gene expression. *Proc. Natl Acad. Sci. USA*, **94**, 814–819.
13. Volfson,D., Marciniak,J., Blake,W.J., Ostroff,N., Tsimring,L.S. and Hasty,J. (2006) Origins of extrinsic variability in eukaryotic gene expression. *Nature*, **439**, 861–864.
14. Pedraza,J.M. and van Oudenaarden,A. (2005) Noise propagation in gene networks. *Science*, **307**, 1965–1969.
15. Weinberger,L.S., Burnett,J.C., Toettcher,J.E., Arkin,A.P. and Schaffer,D.V. (2005) Stochastic gene expression in a lentiviral positive-feedback loop: HIV-1 Tat fluctuations drive phenotypic diversity. *Cell*, **122**, 169–182.
16. Rosenfeld,N., Young,J.W., Alon,U., Swain,P.S. and Elowitz,M.B. (2005) Gene regulation at the single-cell level. *Science*, **307**, 1962–1965.
17. Blake,W.J., Balazsi,G., Kohanski,M.A., Isaacs,F.J., Murphy,K.F., Kuang,Y., Cantor,C.R., Walt,D.R. and Collins,J.J. (2006) Phenotypic consequences of promoter-mediated transcriptional noise. *Mol. Cell*, **24**, 853–865.
18. Raser,J.M. and O'Shea,E.K. (2005) Noise in gene expression: origins, consequences, and control. *Science*, **309**, 2010–2013.
19. Raser,J.M. and O'Shea,E.K. (2004) Control of stochasticity in eukaryotic gene expression. *Science*, **304**, 1811–1814.
20. Rao,C.V., Wolf,D.M. and Arkin,A.P. (2002) Control, exploitation and tolerance of intracellular noise. *Nature*, **420**, 231–237.
21. Elowitz,M.B., Levine,A.J., Siggia,E.D. and Swain,P.S. (2002) Stochastic gene expression in a single cell. *Science*, **297**, 1183–1186.
22. Blake,W.J., Kaern,M., Cantor,C.R. and Collins,J.J. (2003) Noise in eukaryotic gene expression. *Nature*, **422**, 633–637.
23. Kollmann,M., Lovdok,L., Bartholome,K., Timmer,J. and Sourjik,V. (2005) Design principles of a bacterial signalling network. *Nature*, **438**, 504–507.
24. Bengtsson,M., Stahlberg,A., Rorsman,P. and Kubista,M. (2005) Gene expression profiling in single cells from the pancreatic islets of Langerhans reveals lognormal distribution of mRNA levels. *Genome Res.*, **15**, 1388–1392.
25. Raj,A., Peskin,C.S., Tranchina,D., Vargas,D.Y. and Tyagi,S. (2006) Stochastic mRNA synthesis in mammalian cells. *PLoS Biol.*, **4**, e309.
26. Warren,L., Bryder,D., Weissman,I.L. and Quake,S.R. (2006) Transcription factor profiling in individual hematopoietic progenitors by digital RT-PCR. *Proc. Natl Acad. Sci. USA*, **103**, 17807–17812.
27. Chen,J., Germer,S., Higuchi,R., Berkowitz,G., Godbold,J. and Wetmur,J.G. (2002) Kinetic polymerase chain reaction on pooled DNA: a high-throughput, high-efficiency alternative in genetic epidemiological studies. *Cancer Epidemiol. Biomarkers Prev.*, **11**, 131–136.
28. Panne,D., Maniatis,T. and Harrison,S.C. (2007) An atomic model of the interferon-beta enhanceosome. *Cell*, **129**, 1111–1123.
29. Chang,W.L., Baumgarth,N., Yu,D. and Barry,P.A. (2004) Human cytomegalovirus-encoded interleukin-10 homolog inhibits maturation of dendritic cells and alters their functionality. *J. Virol.*, **78**, 8720–8731.
30. Park,M.S., Garcia-Sastre,A., Cros,J.F., Basler,C.F. and Palese,P. (2003) Newcastle disease virus V protein is a determinant of host range restriction. *J. Virol.*, **77**, 9522–9532.
31. Lopez,C.B., Garcia-Sastre,A., Williams,B.R. and Moran,T.M. (2003) Type I interferon induction pathway, but not released interferon, participates in the maturation of dendritic cells induced by negative-strand RNA viruses. *J. Infect. Dis.*, **187**, 1126–1136.
32. Smith,E.S., Li,A.K., Wang,A.M., Gelfand,D.H. and Myers,T.W. (2003) *PCR primer: A laboratory manual*. 2nd edn. Cold Spring Harbor Laboratory Press, Cold Spring Harbor, pp. 211–219.
33. Watson,R.M., Griaznova,O.I., Long,C.M. and Holland,M.J. (2004) Increased sample capacity for genotyping and expression profiling by kinetic polymerase chain reaction. *Anal. Biochem.*, **329**, 58–67.
34. Agalioti,T., Lomvardas,S., Parekh,B., Yie,J., Maniatis,T. and Thanos,D. (2000) Ordered recruitment of chromatin modifying and general transcription factors to the IFN-beta promoter. *Cell*, **103**, 667–678.
35. Thanos,D. and Maniatis,T. (1992) The high mobility group protein HMG I(Y) is required for NF-kappa B-dependent virus induction of the human IFN-beta gene. *Cell*, **71**, 777–789.
36. Munshi,N., Yie,Y., Merika,M., Senger,K., Lomvardas,S., Agalioti,T. and Thanos,D. (1999) The IFN-beta enhancer: a paradigm for understanding activation and repression of inducible gene expression. *Cold Spring Harb. Symp. Quant. Biol.*, **64**, 149–159.
37. Gillespie,D.T. (1977) Exact stochastic simulation of coupled chemical reactions. *J. Phys. Chem.*, **81**, 2340–2361.
38. Frevel,M.A., Bakheet,T., Silva,A.M., Hissong,J.G., Khabar,K.S. and Williams,B.R. (2003) p38 Mitogen-activated protein kinase-dependent and -independent signaling of mRNA stability of AU-rich element-containing transcripts. *Mol. Cell. Biol.*, **23**, 425–436.
39. Whittemore,L.A. and Maniatis,T. (1990) Postinduction turnoff of beta-interferon gene expression. *Mol. Cell. Biol.*, **10**, 1329–1337.
40. Pastinen,T. and Hudson,T.J. (2004) Cis-acting regulatory variation in the human genome. *Science*, **306**, 647–650.